On the electronic structure of REE bearing crystalline compounds and silicate glasses determined by RIXS

[1]S. Simon, [1]M. Wilke, [2]S. Klemme, [3]W. A. Caliebe, [4]K. Kvashnina

[1] Deutsches GeoForschungsZentrum GFZ, Potsdam, Germany (*correspondence: **ssimon@gfz-potsdam.de**), [2] Westfälische Wilhelms-Universität, Münster, Germany, [3] Deutsches Elektronen-Synchrotron, Hamburg, Germany, [4] European Synchrotron Radiation Facility, Grenoble,France

MOTIVATION

Core level spectroscopy has gained interest in earth science in the last decade because it provides deep insight into the electronic structure of elements in mineral phases (crystalline and non-crystalline) and thus, their coordination environment. In resonant inelastic x-ray scattering (RIXS) a core-electron is promoted to an excited state just as in XANES but also the energy dependence of the scattered or emitted photon is measured, which gives additional information about the intermediate and the final state (Fig. 1, 3). Here we present high resolution (HR) XANES and RIXS spectra of rare earth elements (REE) in minerals and melts. The electronic structure of REE is mainly determined by the interactions between electrons in the localized 4f and in the broad 5d bands.

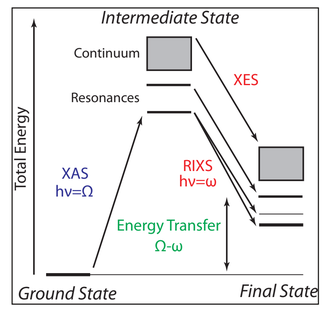

Fig. 1: RIXS energy scheme.

Application: Effect of silicate glass composition on coordination of REE.

EXPERIMENTAL

- Melt compositions, taken from [2] as well as simplified natural compositions (haplogranite and haplobasalt), were doped with selected REE (La (0.5 wt%), Gd (0.5 wt%), Yb (2 wt%)) and synthesized as glasses. Compositions [2] and simplified natural compositions vary in the aluminum saturation index (ASI: molar radio of $Al_2O_3/(Na_2O+K_2O+CaO)$) and thus in polymerisation.
- Yb-2p3d RIXS and HR-XANES was collected at beamline W1 (DESY) using the high resolution WDX spectrometer in Johann geometry. La and Gd-2p3d RIXS and HR-XANES were collected at beamline ID 26 (ESRF) using the high resolution WDX spectrometer in Rowland geometry (Fig. 2). Rowland circle was 1m for both setups.

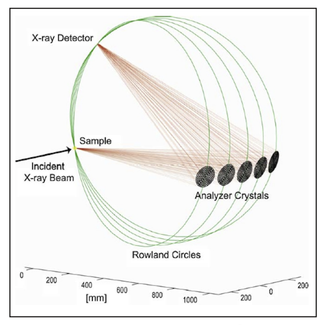

Fig. 2: Setup of WDX spectrometer at ID 26.

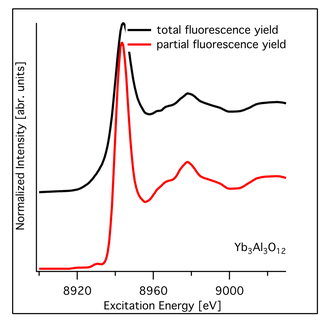

Fig. 3: PTY vs. TFY for $Yb_3AL_5O_{12}$.

RESULTS - HR-XANES

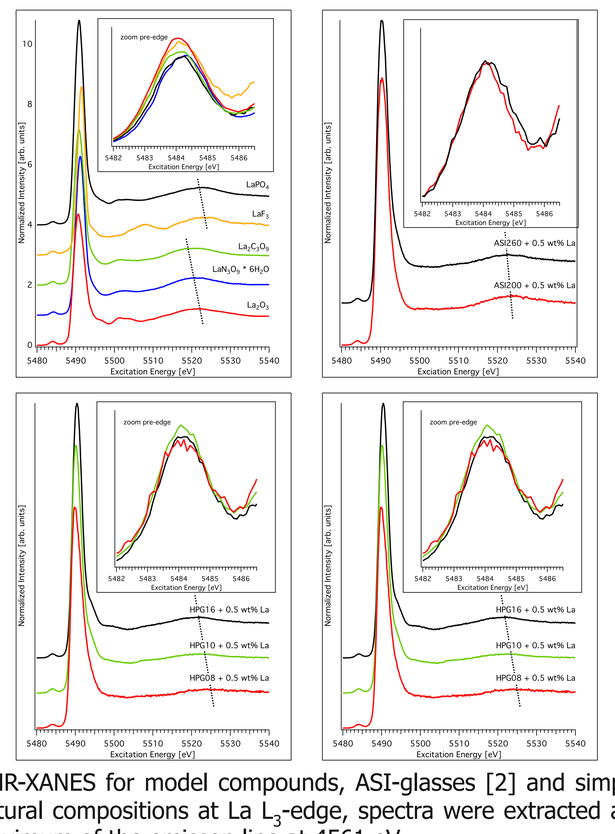

Fig. 4: HR-XANES for model compounds, ASI-glasses [2] and simplified natural compositions at La L_3-edge, spectra were extracted at the maximum of the emisson line at 4561 eV .

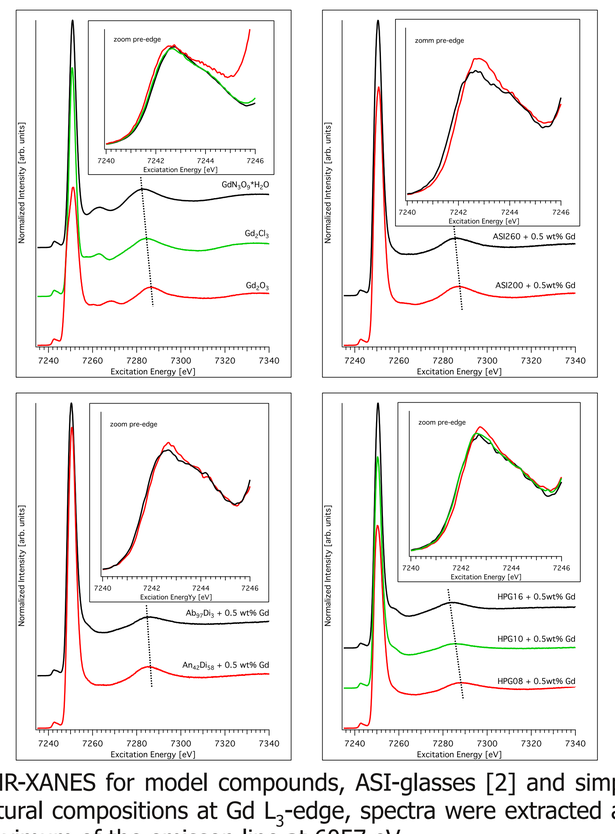

Fig. 5: HR-XANES for model compounds, ASI-glasses [2] and simplified natural compositions at Gd L_3-edge, spectra were extracted at the maximum of the emisson line at 6057 eV .

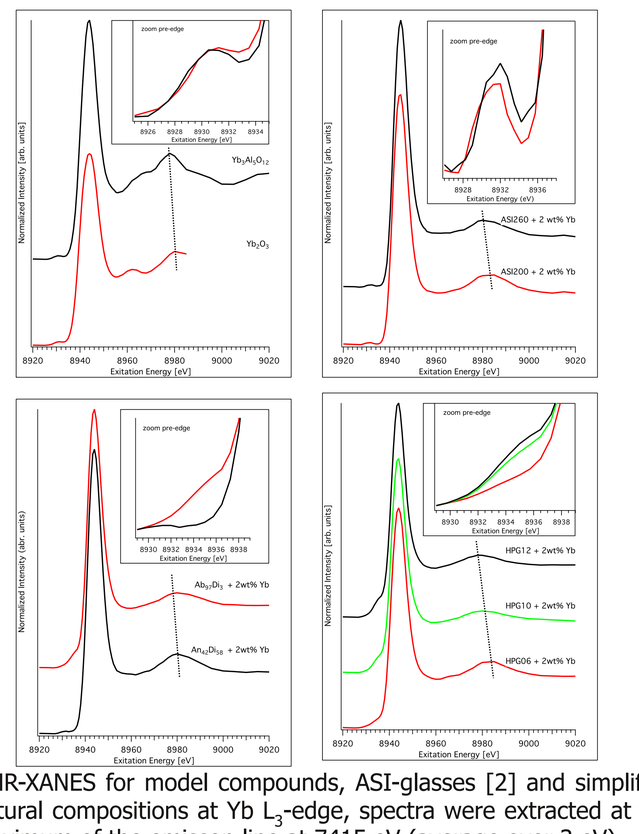

Fig. 6: HR-XANES for model compounds, ASI-glasses [2] and simplified natural compositions at Yb L_3-edge, spectra were extracted at the maximum of the emisson line at 7415 eV (average over 3 eV).

RESULTS - RIXS

Electron Configuration La: [Xe] $6s^2$ $5d^1$

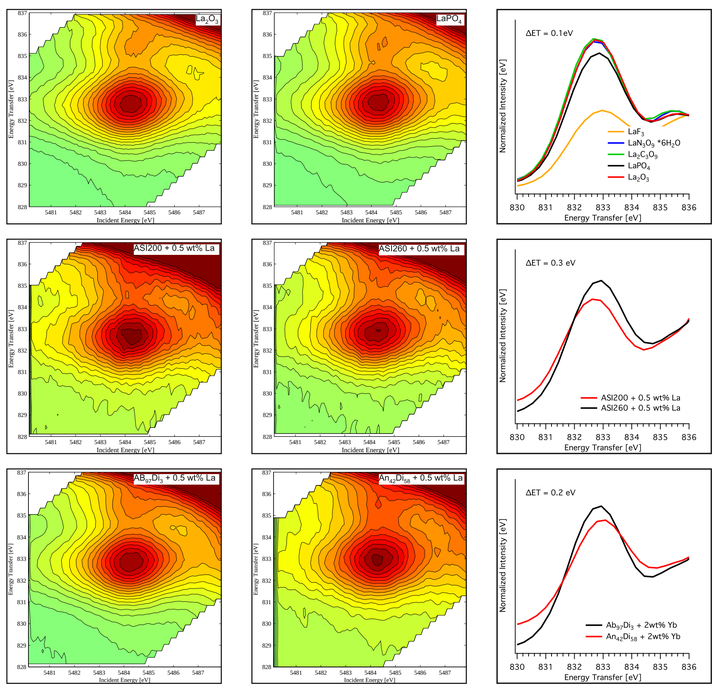

Fig. 7: left, 2p3d RIXS intensity map of the pre-edge region at the La L_3-edge for the model compounds, ASI-glasses [2] and simplified natural compositions; right, cross section along energy transfer (ET) at the maximum of the exciation energy (average 3eV).

Electron Configuration Gd: [Xe] $6s^2$ $4f^7$ $5d^1$

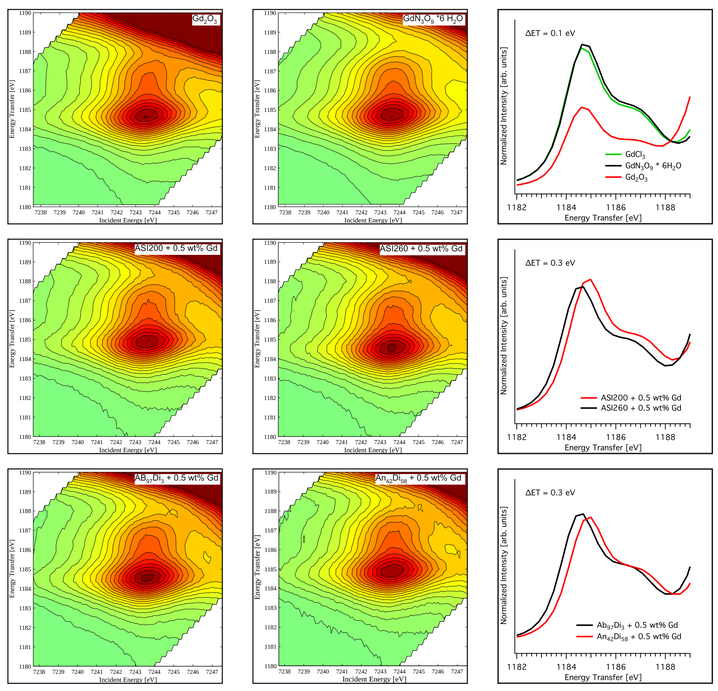

Fig. 8: left, 2p3d RIXS intensity map of the pre-edge region at the Gd L_3-edge for the model compounds, ASI-glases [2] and simplified natural compositions; right, cross section along energy transfer at the maximum exciation energy (average. 3eV).

Electron Configuration Yb: [Xe] $6s^2$ $4f^{14}$

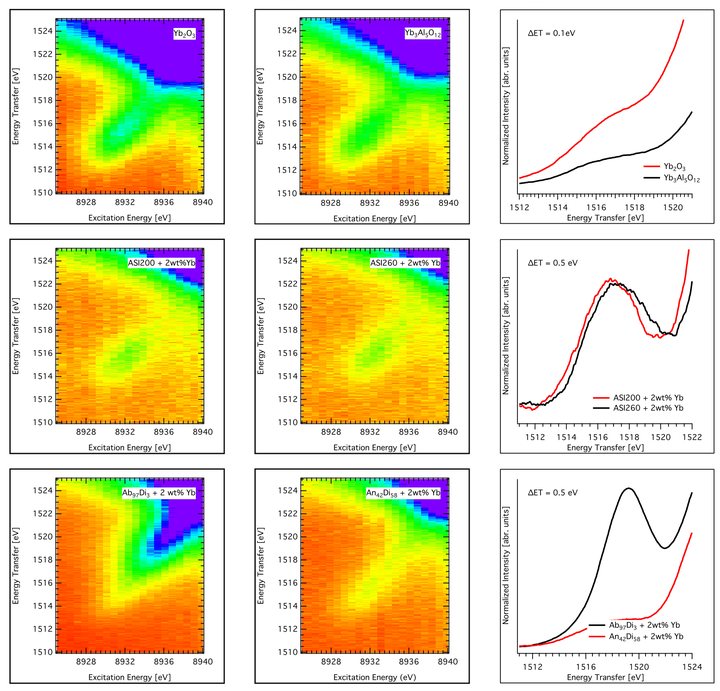

Fig. 9: left, 2p3d RIXS intensity map of the pre-edge region at the Yb L_3-edge for the model compounds, ASI-glases [2] and simplified natural compositions; right, cross section along energy transfer at the maximum exciation energy (average 3eV).

CONCLUSION

- Results derived by EXAFS suggest that the local structure around REE changes with increasing of melt polymerization. E. g. the average Y-O distance changes from 2.27 Å to 2.39 Å and the number of neighbours increases from 6 to 8 for a change in ASI from 0.115 to 0.768 [4]. EXAFS data at the L_3-edge of Gd and Yb show similar trends. The lower amount of non-bridging oxygens in melts with ASI≈1 forces Y to bond to bridging oxygens at longer distances and coordination number to meet local charge balance requirements.
- Partial fluorescences HR-XANES (Fig. 4, 5, 6) spectra indicate a change of the coordination supported by a shift of the first EXAFS maximum. 2p3d RIXS maps of the pre-edge region show an increase of the pre-edge and a slight shift of the maximum energy tranfer to higher energies for La (Fig. 7) and Yb (Fig. 9) with increase of ASI. For Gd (Fig. 8), a decrease of the pre-edge intensity and a slight shift of the maximum energy tranfer to lower energies with increase of ASI is observed. Difference in electron configuration and orbital hybridisation may explain different behavior of the pre-edge.

References:

[1] Blundy & Wood (2003) Earth Planet. Sci. Lett. 210, 383- 397. [2] Prowatke & Klemme (2005) Geochim. Cosmochim. Acta 69, 695-709. [3] Ponader & Brown (1989) Geochim. Cosmochim. Acta 53, 2893-2903. [4] Simon et.al Abstract 481